Progress Report

Giant Magnetoresistive Sensors
A Phase II SBIR
Contract N00012-96C-0342

To

Dr. Larry Cooper
Office of Naval Research

From

Nonvolatile Electronics, Inc.
11409 Valley View Road
Eden Prairie, MN 55344

Period of Performance:
15 August 1996 Through 15 August 1998

Report Covers Period:
15 November 1996 Through 15 May 1997

James M. Daughton, Principal Investigator
Mark Tondra, Senior Physicist
(612)996-1607 Phone
(612)996-1600 Fax
daughton@nve.com email

Progress Report

Giant Magnetoresistive Sensors

J.M. Daughton, PI
Mark Tondra

1) Program Overview

This report covers the period from November 15, 1996 to May 15, 1997 - from month 4 through month 9 of the program. This period has concentrated on the design of the sensor and corresponding improvements required in the tunneling device materials and in demonstrating the feasibility of a superior mode of operation. A design has been completed and is in process. Measurements made on devices indicate that the design should achieve a sensitivity to magnetic fields of lower than 10^{-7} Oe. By the end of the first year of the program, we are to be in position to make a hybrid circuit (breadboard) version of the sensor, and based on the results of the first nine months of the program, we should be able to meet that goal.

Progress in developing SDT materials with antiferromagnetic pinning has been good, and a current capability to deposit them with relative ease has been demonstrated. An ion milling process was devised to overcome a problem encountered with the iron manganese antiferromagnetic material being ultra-sensitive to chemical etching. The new pinning ideas using a Co-Ru-Co antiferromagnetic-coupled pair worked as predicted. A sputtering target of iridium manganese has been ordered, and the substitution of this material for iron manganese should improve higher temperature operation of the sensor.

Noise and measurements on pinned tunneling samples of approximately the correct size showed the noise to be less than ten times the Johnson noise floor, and at least some of the noise observed is due to the experimental setup. Signal measurements showed about 3% per Oe sensitivity in a linear region of operation as predicted, and somewhat better sensitivity should be achievable with the devices in fabrication. Series strings of tunneling sensor elements allowed higher operating voltages with high GMR and showed break-down voltages approximately proportional to the number of individual elements.

A full mask set has been designed and devices are in process to test the performance of completed devices against program goals.

Spending on this program is approximately on plan and consistent with accomplishments to date. Basic processing and materials work has been completed, and the remaining program will be primarily processing and testing. Through April, 1997 (8 1/2 months) the program has been billed $286,688 out of

an anticipated $749,784 30 month program (assuming the six month option for $149,794 is exercised for an integrated sensor demonstration). At this point it is anticipated that the contract will be completed on time and on cost.

This report is a summary of results to date, and includes 2) materials improvements, 3) sensor mode testing, 4) sensor layout, 5) full output bridge design, 6) upper limit on noise floor, 7) process development, and 8) test apparatus design.

2) Material improvements

Since our last report, many improvements have been made in the basic material properties of the Spin Dependent Tunneling (SDT) structures. Our results are summarized in the following table. The "Best Value" column lists the best results from many different wafers. The "Predicted" column describes the properties we believe are achievable in a single wafer.

Parameter	Best Value	Predicted
JMR (%)	24%	>= 24%
Soft axis coercivity	3 Oe	< 5 Oe
Soft axis hysteresis	3 Oe	< 10 Oe
Soft axis offset	0 Oe	< 5 Oe
Tunnel resistivity	0.1 MW-mm^2	< 0.5 MW-mm^2
Hard layer pinning	> 1000 Oe	> 1000 Oe
Resistive thermal coef.	-0.1% / ^{0}C (25 to 125 ^{0}C)	-0.1% / ^{0}C (25 to 125 ^{0}C)
Thermal signal degradation	0.1% / ^{0}C (25 to 125 ^{0}C)	0.1% / ^{0}C (25 to 125 ^{0}C)
Max operating temp	125 ^{0}C	>125 ^{0}C
Max storage temp	200 ^{0}C	>200 ^{0}C

There are some tradeoffs evident going from "Best Value" to "Predicted" wafers. The most significant one has to do with the relationship between coupling between the top and bottom magnetic electrodes and the thickness of the barrier between them. A thinner barrier results in lower resistivity and usually a higher JMR, but at the cost of higher interlayer coupling. Another tradeoff is between low resistivity and device integrity. In order to get lower than 0.1 MW-mm^2 resistivity, the Al_2O_3 barrier must be thinner than 16Å. But as the barrier gets thinner, chances of getting pinhole defects from deposition or migration grow.

From this table, it is apparent that the development of our raw SDT material is largely complete. It should be noted that our confidence in producing SDT wafers has grown dramatically in recent months. We are capable of naming desired values for various parameters, designing a structure to get those properties, and building a wafer with a high probability of success.

At the time of our first report, we had identified the best way to grow the Al_2O_3 barriers: put down a layer of pure Al, and then deposit some more Al in an oxygenated plasma. (This mode of deposition was suggested by Dr. Jagadeesh Moodera of MIT). This special oxidation technique has two phases: an initial rapid oxidation and a subsequent slow oxygen diffusion. For a given barrier thickness, there is an optimal set of plain and oxidized Al deposition steps such that as much of the deposited Al is oxidized without allowing the underlying magnetic material to be oxidized. Several experiments have been carried out to understand these fine points. One of particular interest was a sweep of

oxygenated deposition after a fixed pure Al deposition thickness. The structures of these wafers was NiFeCo 125 / Al 12 / Alox X / CoFe 125, where X is the thickness of the oxygenated Al deposition. As was expected, the tunnel resistivity increased with X.

3) Sensor mode testing

The last report described a mode of sensor operation where one of the two magnetic layers is pinned along the easy (sensitive) direction while the soft (active) layer is biased perpendicular to the easy direction. Based on work done since the last report, we believe this sensor mode will be successful. We have succeeded in fabricating pinned SDT devices, which is a major achievement for us due to particular processing difficulties discussed in the "Process Development" section below. In addition, we were able to test the sensor mode by using a permanent magnet for the orthogonal biasing. In this preliminary test, we were able to achieve a 3% / Oe sensitivity in zero ambient field. We expect that with more precise field biasing and somewhat better starting SDT material, it will be possible to achieve a 20% / Oe zero field sensitivity as predicted in our previous report. What follows in this section will describe the SDT material and the sensor mode in more detail.

Figure 1 shows a schematic cross section of a pinned SDT device. The tunnel junction is the same as our basic SDT device in that it's an Al_2O_3 barrier with NiFeCo on one side and CoFe on the other. But in this special pinned structure, there is a tightly antiparallelly coupled CoFe sandwich pinned by FeMn. The sandwich has several advantages as a "hard" layer over a typical CoFe layer pinned with FeMn. For one, the net moment of the sandwich is relatively low, so external fields have a lesser effect on the sandwich as a whole. The temperature stability of the Ru coupling is very good, which helps extend the upper limits of the FeMn pinning. And the CoFe sandwich has natural flux closure which should reduce coupling between the top and bottom electrodes.

The data we have collected on these structures is quite exciting. In particular, the JMR is around 20% for a wide range of device sizes and shapes. And the soft layer switching occurs at 4 to 11 Oe. Also, the interlayer coupling is well below 5 Oe. Figure 2 gives a representative sample of this behavior.

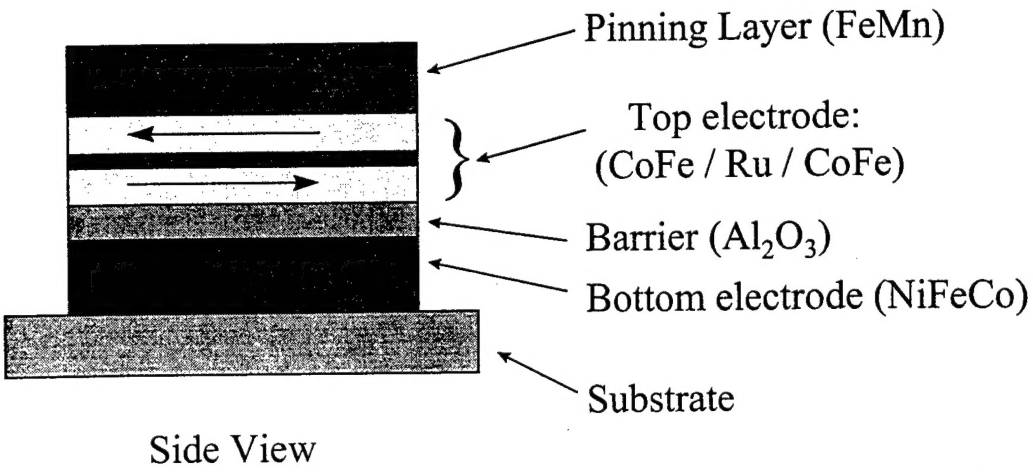

Fig. 1: Cross section of a pinned SDT device with the top electrode being a CoFe/Ru sandwich. Typical layer thicknesses are NiFeCo 125 / Al_2O_3 20 / CoFe 70 / Ru 9 / CoFe 70 / FeMn 125.

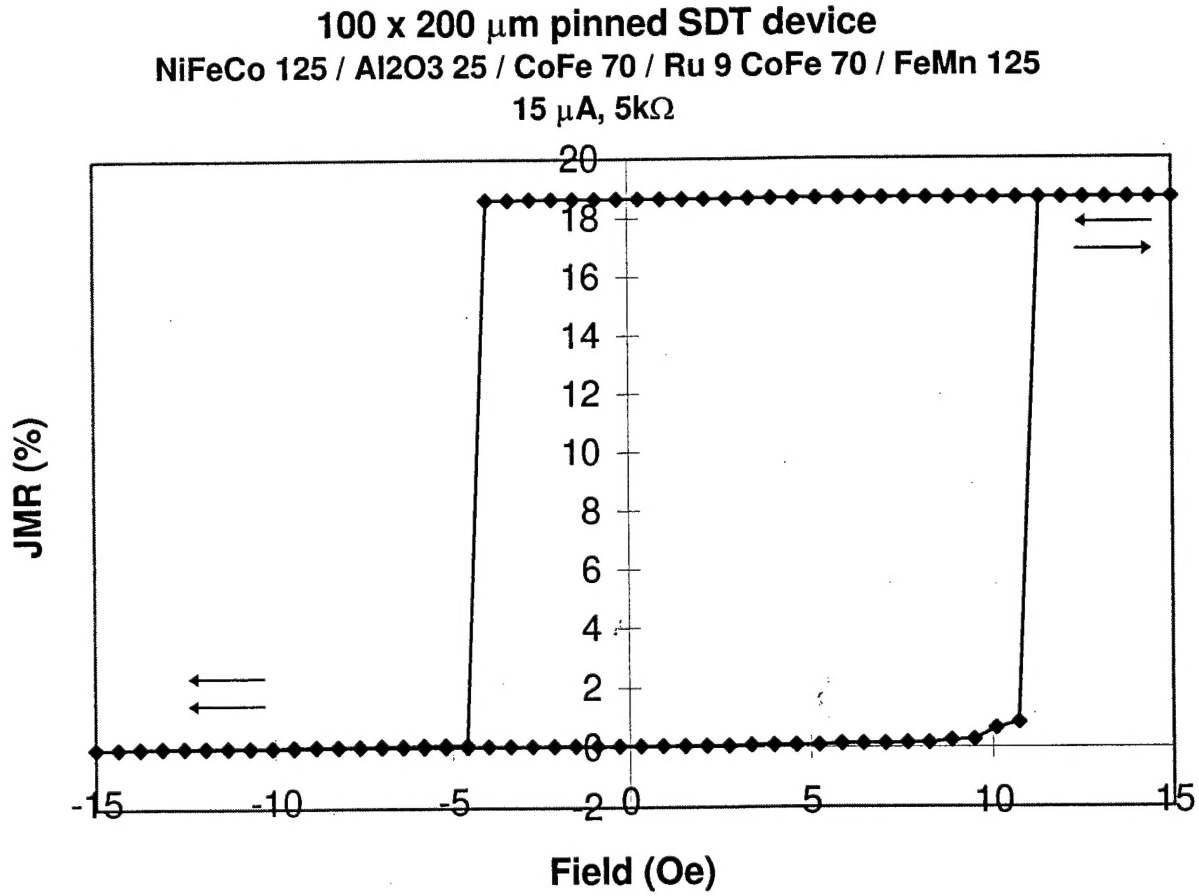

Figure 2: Magnetoresistive data from a fairly large SDT device. Typically, an unpinned device that was this big would have less than the maximum JMR because the completely antiparallel magnetic state would never be realized. The applied field is parallel to the pinned direction.

These data show that the soft layer switches very quickly and uniformly. Data collected with a denser field spacing indicate that the entire switch takes place in less than 100 mOe. Unfortunately, the absolute value of the switching field ranges over a few Oe from sweep to sweep, and this switching is believed to have a noisy signal. So, we still need the hard axis biasing scheme to make a sensor out of this SDT material. The biasing scheme, discussed at length in the last report, is depicted below.

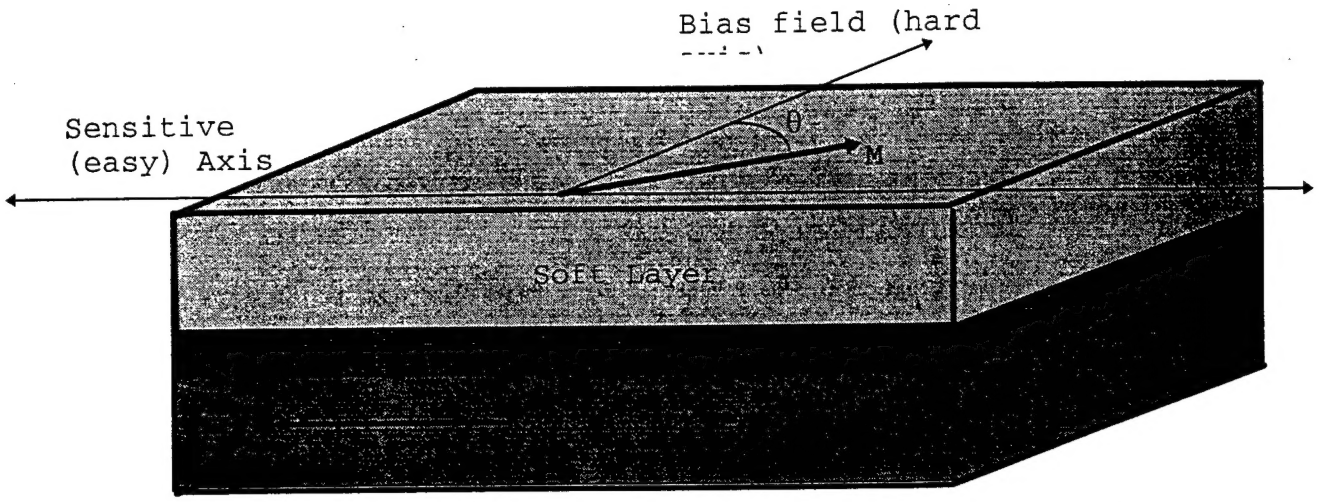

Figure 3: Hard axis bias sensor mode. The magnetization of the soft layer rotates in the film plane while the pinned layer's magnetization is fixed. The output goes as sin q.

The data in Figure 4 were collected from a device on the wafer with a permanent magnet about 50mm above the wafer. The magnitude of the field was on the order of 10's of Oe. The magnet was oriented such that most of the field was perpendicular to the sensitive axis, but rotated just enough so that the interlayer coupling was canceled by the easy axis component.

4) Sensor layout

The data shown here have been collected from single SDT elements. We have, however, completed layout and mask construction for complete biased bridges of multiple element arrays of SDT elements. Wafers using this layout are in process now. The sensor design was described in some detail in our first report, but there are some key features worth reviewing. First is the fact that arrays of SDT elements are being used for each of the four sensor bridge elements. This is because the JMR as a percent of total signal drops with increasing element voltage. In practical terms, each element needs to operate at about 100mV or less. So to get a reasonable signal and to boost the signal to noise ratio, it is advantageous to string many elements together to increase the total signal. This

is analogous to making a long, serpentine conduction path in metal to increase the resistance. The arrays in the present design have 16 elements per bridge leg, though there is no reason why more couldn't be added if a higher operating voltage were available. In fact, since the signal to noise ratio goes up as $R^{1/2}$, more elements are better. This assumes that wafer space is not a critical issue.

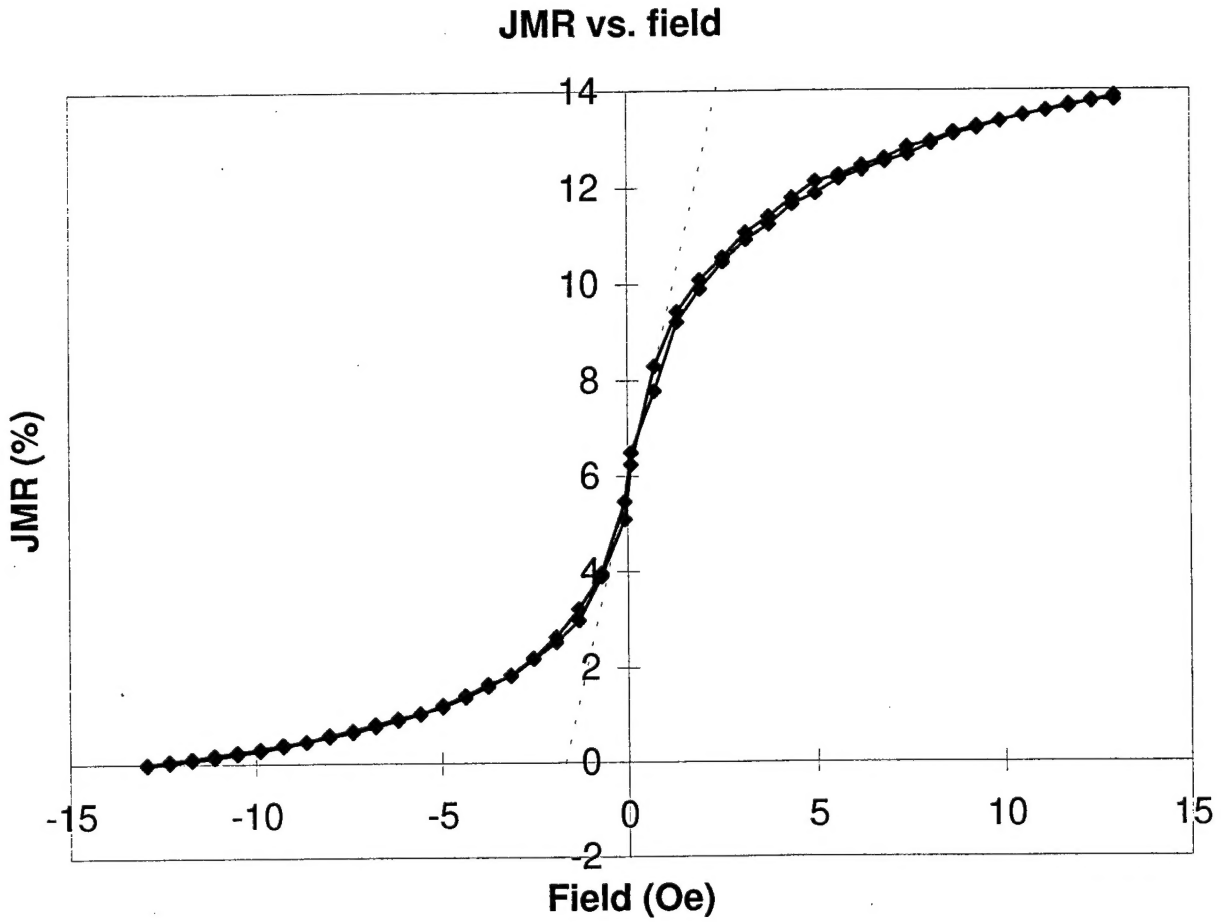

Figure 4: The pinned SDT device with an externally applied hard axis bias. The field is being swept along the easy axis of the soft layer, and the hard layer is pinned in the negative direction, parallel to the easy axis. The dotted line, inserted as a guide to the eye, corresponds to a sensitivity of roughly 3%/Oe.

Other key features of the sensor design are the two sets of integrated bias straps. Currents passed through these straps generate magnetic fields in the plane of the sensor films and perpendicular to the strap length. One set of straps is designed to provide the hard axis bias for the soft layer. The other set is for setting the initial pinning direction for the different bridge legs and for applying a small reverse field along the easy axis to compensate for any coupling between the hard and soft layer. This coupling acts as a small easy

axis offset, as evident in Figure 2. Pictures of a single array, a bridge of arrays, and the total sensor layouts are included in Figures 5, 6, and 7.

It is interesting to note that this bridge design has several built in noise immunities. First is the usual immunity to bridge excitation current. As long as the bridge is balanced, there will be equal currents flowing through both sides of the bridge regardless of the total current level. Second is the easy axis biasing. The coils are arranged so that opposite legs of the bridge feel oppositely directed easy axis bias fields. Since opposite legs also have oppositely pinned hard layers, they have opposite sign of MR slopes. The net effect is that equal but opposite noise on the easy axis bias straps cancels out in the bridge. Third is the hard axis biasing. Noise in the bias strap here has the effect of changing the slope of the MR response. An increase in bias current results in a decrease in slope of equal magnitude in all four legs of the bridge. While this symmetry does not completely cancel out the noise, it is of some help.

5) Full Output Bridge Design

Dr. Dexin Wang was responsible for a significant innovation in bridge sensor design. Specifically, he devised a way to have opposite legs of the bridge pinned in opposite directions without relying on bias straps. The key to the idea is the use of a "synthetic antiferromagnet" layer in the top electrodes of one pair of bridge legs. The antiferromagnetic layer is simply a CoFe / Ru / CoFe sandwich with unequal layers of CoFe. The Ru keeps the two CoFe layers tightly antiparallel, but doesn't have any effect on the direction and orientation of the net moment of the sandwich. An external magnetic field, then, causes the net moment of the sandwich to rotate towards the applied field. If the top CoFe layer in the sandwich is thicker than the bottom layer, the top layer becomes parallel to the external field while the bottom layer becomes antiparallel. Conversely, if the bottom layer is thicker, the roles are reversed, and the bottom layer is parallel while the top layer is antiparallel to the applied field. Using this fact, a bridge can be constructed so that the CoFe layer which forms the upper electrode of the SDT device is pinned in opposite directions on opposite bridge legs. The usual way to do this is to heat the sample up past the Neel temperature of the FeMn pinning material, and then cool it down while passing current through the easy axis bias straps. This new way requires only that there be a field applied while the FeMn is being deposited. Figure 8 shows how the CoFe / Ru sandwiches are pinned by FeMn when a field is applied during deposition.

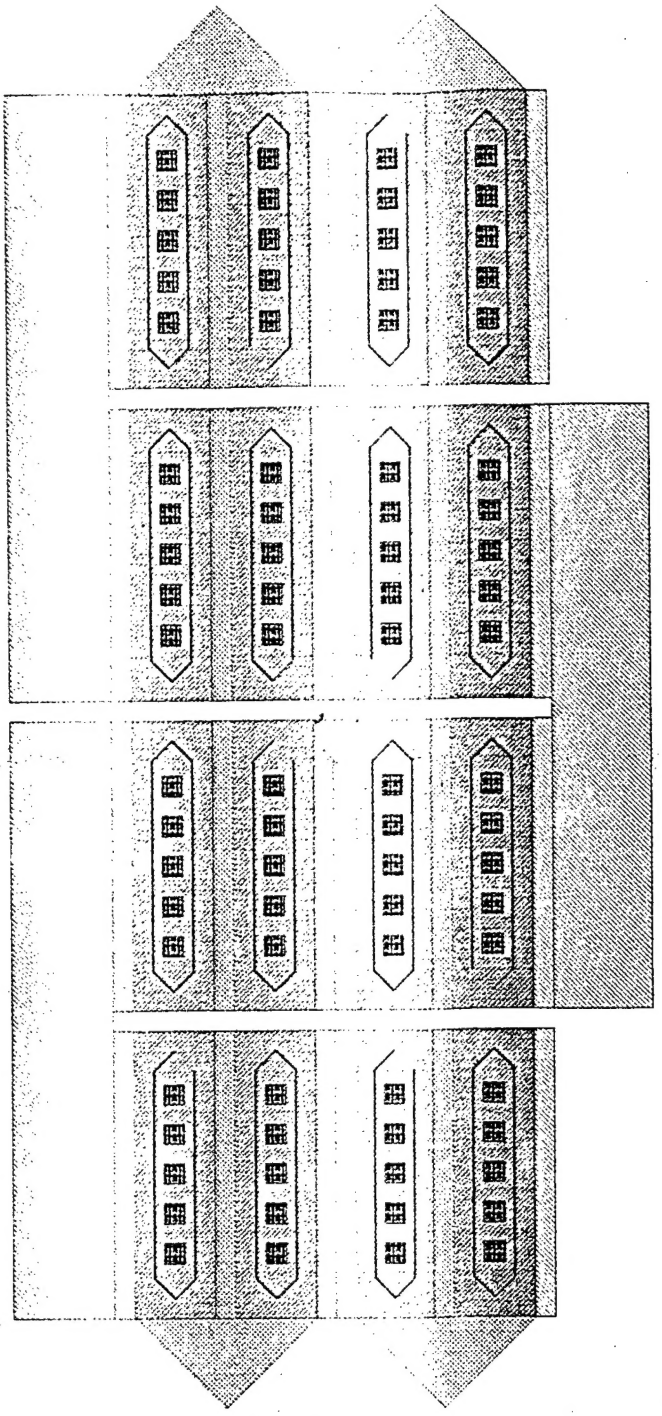

Figure 5: An array of 16 SDT elements

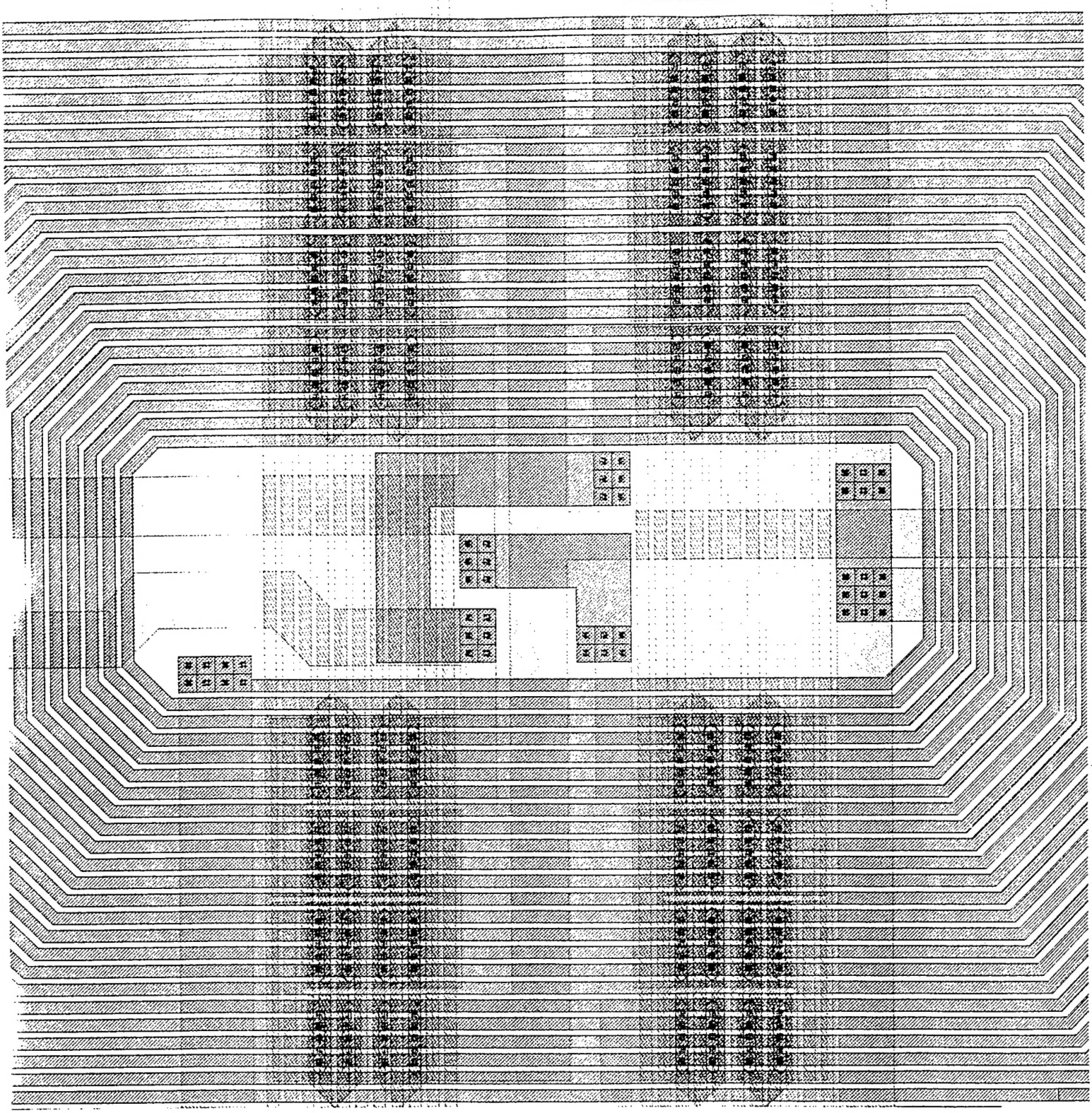

Figure 6: A bridge of four 16 SDT element arrays.

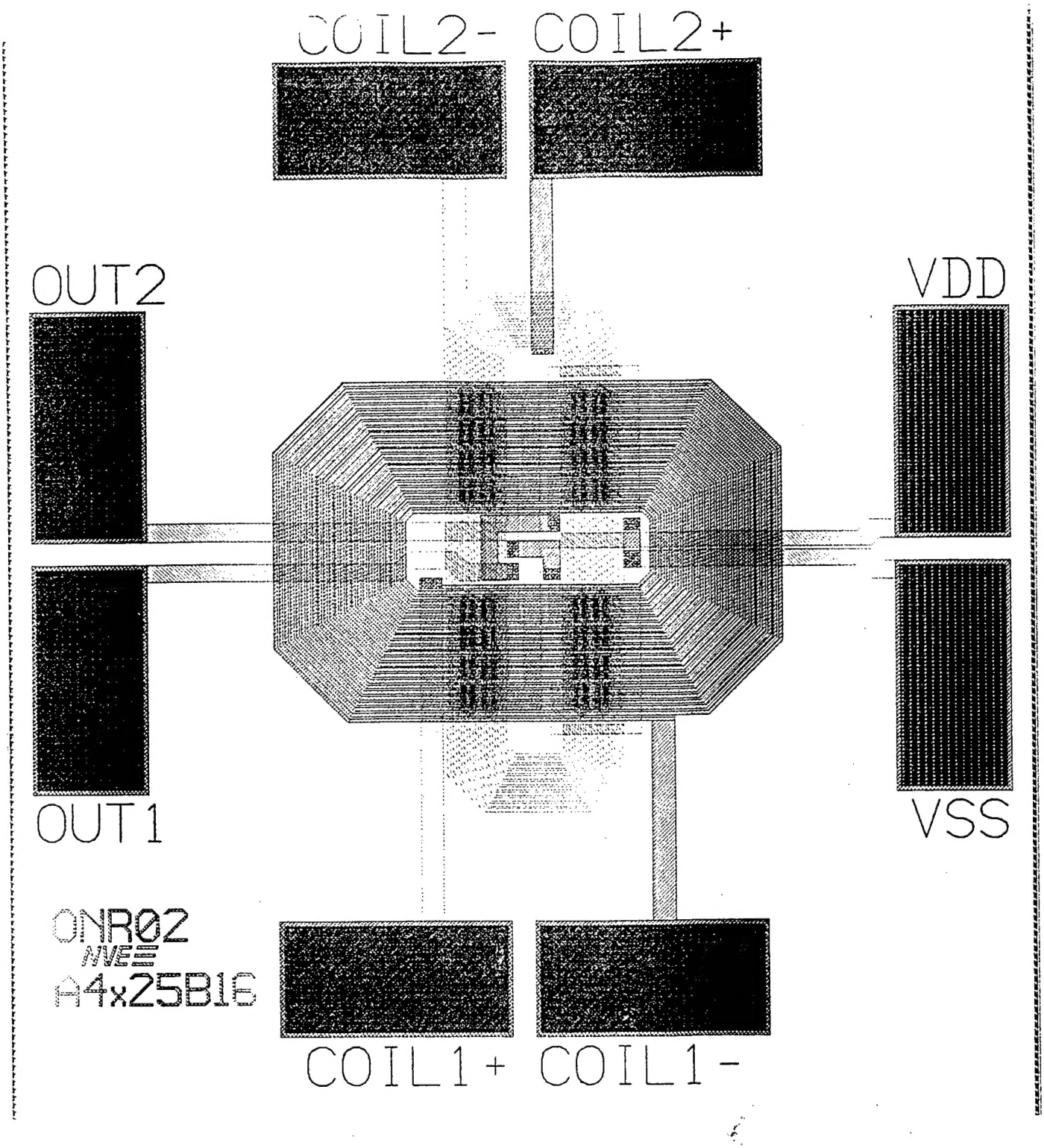

Figure 7: The full sensor layout with two sets of biasing coils.

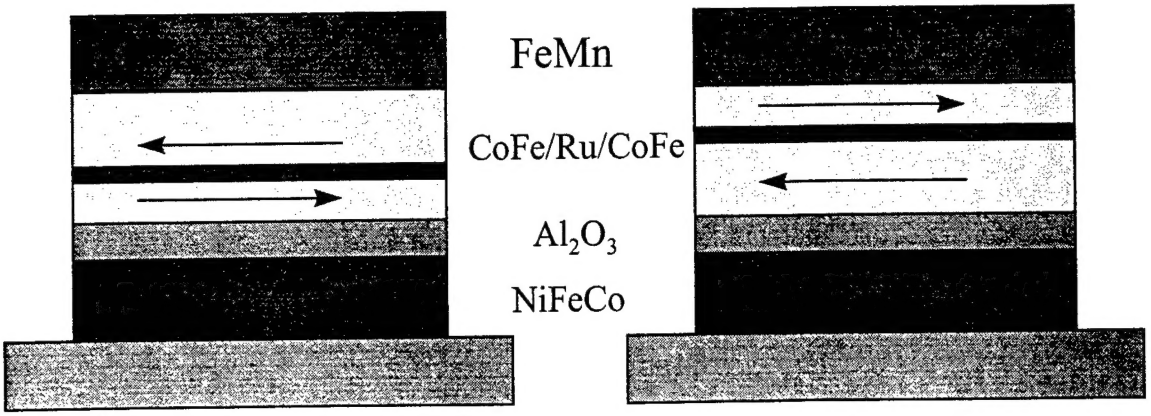

Figure 8: This is how the two types of stacks would be pinned if a field was applied to the left while the FeMn was being deposited.

6) Upper limit on noise floor established

Preliminary noise measurements have been made to determine the fundamental noise floor for the sensor mode described above. The experiment was done on a number of different devices whose area and total resistance ranged over several orders of magnitude. Before discussing the experimental details, the bottom line is that the measured noise was between 5 and 10 times Johnson noise for all devices. Given that no effort was made to electrically shield the devices and that the sensor biasing was primitive, these measurements are only an upper limit on the material noise and not the absolute floor. Thus, it appears that we should be able to achieve a *basic material* signal to noise ratio required for a 10^{-7} to 10^{-8} Oe sensor. Needless to say, other sources of noise in the sensor circuit may be the limiting factor of ultimate sensor resolution.

The noise spectral density was measured using an HP3582A Spectrum Analyzer. For the sake of consistency, all the measurements were taken at 208 Hz with a spectral range of 1000 Hz with a bandwidth of 6 Hz. 208 Hz is a relatively quiet region of this frequency range. It should be noted that, since the samples were still in wafer form, it was impossible to make a measurement in a shielded environment.

Though the measurements were taken from devices on a wafer, actual device operating conditions were simulated using an external permanent magnet to provide the required hard axis bias to the soft magnetic layer. Once the permanent magnet was positioned to bias the device to an optimally sensitive point, the noise data were taken with no additional applied field.

7) Process development

At last report, it was determined that some sort of pinning was required to achieve the desired material sensitivity. This presented a large practical difficulty in processing the SDT devices. This is because typical pinning materials, and FeMn in particular, are not compatible with the wet etch technique we were using for forming the top electrode of our SDT devices. Several possible solutions to this problem were identified, and one of those has proven to be quite successful.

The best solution is to replace the wet etch of the top electrode with an ion mill etch. The difficulty here is that there is no practical etch stop for the ion mill (the Al_2O_3 barrier serves as the etch stop for the wet technique). Consequently, the effort was in learning how to predict and measure the progress of the ion mill etch. We now have depth control of this process to about 20Å.

A second process, which has not been employed with the SDT devices but has very broad applicability, is a tungsten lift-off procedure. The key idea here is that W etches easily in H_2O_2 while the other materials in GMR structures don't. Also, W will not cause a contamination problem in the sputtering system while normal photoresist will. The process steps are: 1) deposit desired underlayers, 2) deposit about 5000Å W, 3) pattern photoresist on the W such that the W is exposed where subsequent structures are desired, 4) etch the W "window with an ion mill, RIE, or H_2O_2, 5) deposit the desired structure in the hole, and 6) remove W in an H_2O_2 bath.

8) Test apparatus design

A three-axis helmholtz coil arrangement has been designed, machined, and is nearly complete. This apparatus, when placed inside our zero-gauss chamber, will allow us to test and evaluate sensors to the required precision. The coils are large enough that there will be a region of pT uniformity several mm on a side. Each coil will actually consist of three co-axial windings so that one can simulate an ambient external field, an internal feedback or biasing field, and a perturbation field, all with appropriate precision. Samples being placed in the coils for testing are mounted on an extension to the lid such that proper orientation is achieved each time.